Desalination and Water Treatment
www.deswater.com

doi:10.5004/dwt.2019.24331

165 (2019) 301–313
October

Kinetics modeling and experimental validation of Reactive Blue 5G dye removal from synthetic solution by electrocoagulation

Claudia Luiza Manfredi Gasparovic*, Eduardo Eyng, Laercio Mantovani Frare, Fabio Orssatto, Larissa de Bortoli Chiamolera Sabbi, Ilton José Baraldi

Federal University of Technology – Parana, Brazil Avenue, 4232, Zip Code 85804-000, Medianeira, Parana State, Brazil, email: claudiag@alunos.utfpr.edu.br (C.L.M. Gasparovic), eduardoeyng@utfpr.edu.br (E. Eyng), laercio@utfpr.edu.br (L.M. Frare), orssatto@utfpr.edu.br, (F. Orssatto), larissasabbi@utfpr.edu.br (L.B.C. Sabbi), baraldi@utfpr.edu.br (I.J. Baraldi)

Received 10 January 2019; Accepted 29 April 2019

ABSTRACT

The main contribution of this work was to obtain a model for the removal kinetics of reactive Blue 5G dye from synthetic effluents by electrocoagulation with iron electrodes and carry out its experimental validation, which often is a neglected step. Experiments were conducted using a batch electrocoagulation system, with dye concentration and the intensity of electric current applied to the electrodes as variables, while dye and iron concentrations were determined from samples taken over time. The kinetics of the process was modelled with commonly used kinetics models, as well as sigmoidal models. Good fits were obtained for all the models tested ($R^2 > 90\%$). However, the experimental validation of the fitted models showed that the sigmoidal logistic model presented the best performance among those tested. Therefore, this model can be used to simulate the decay of the concentration of reactive Blue 5G dye throughout the process, something that was not possible using the adsorption models. A thermodynamic analysis was conducted with the experimental results, in which the entropy generation of the process was calculated. This analysis allowed to discuss possible reasons for sigmoid models presenting a better fit than the usually employed adsorption curves.

Keywords: Electrochemical treatment; Kinetic modeling; Sigmoidal models; Textile wastewater

1. Introduction

The textile industry generates large quantities of liquid effluents [1–3], which present high polluting potential [4,5], due to high levels of chemical oxygen demand (COD), total organic carbon, salinity, large amounts of suspended solids (SS) and heavy metal ions, biotoxicity, and specially, strong color due to the presence of dyes [6–10].

Azo dyes, which have been extensively used, stand out among the different types of dyes [11]. They have recalcitrant characteristics that make removal a challenging task, thus motivating the need for innovative approaches to treatment [12].

Conventional treatment of these effluents can be achieved by biological oxidation, chemical coagulation, precipitation and adsorption, and advanced techniques are also currently employed, such as ultrafiltration and advanced oxidation processes, which include ozonization, Fenton and photo-Fenton processes, photolysis with H_2O_2 and O_3 [13–15], each presenting some disadvantages [16].

Many of these processes, including advanced oxidation processes such as ozone, photochemical, Fenton's, take considerable time, required expensive setup and are not applicable for small plants [17]. Adsorption and precipitation processes are very time-consuming and expensive, presenting low efficiency [18]. Overall, the costs of adsorption, ultrafiltration and ozonization usually exceed that of chemical coagulation. However, when chemical coagulation is used to treat dyed wastewaters, secondary pollution occurs due to the high quantities of chemical substance added at a high concentration [14].

Chemical degradation by oxidative agents are among the most effective methods, however it can produce toxic

*Corresponding author.

products such as organochlorine compounds [13]. Photooxidation by UV/$_2O_2$ or UV/TiO_2 needs additional chemicals, and therefore also causes a secondary pollution. Although biodegradation process is cheaper than other methods, it is less effective because of the toxicity of dyes that has an inhibiting effect on the bacterial development [19].

In this context, electrocoagulation has emerged as an interesting technological alternative [4], because its ease of operation, lower sludge generation and no requirement for chemicals addition [16,20]. Electrocoagulation also presents high efficiency in the removal of color and complex effluents treatment, such as those of the textile industry [21].

Electrocoagulation consists of a complex process in which coagulant ions are produced *in situ* by applying electric current to sacrificial electrodes. The ions destabilize contaminants particles, which then aggregate into flakes [20,22]. Simultaneously, gas bubbles are generated at the cathode, which results in the flotation of the newly formed flakes [23–25].

There are many different mechanisms for dye removal with electrocoagulation that are proposed in literature. According to [26,27], two main mechanisms for removing dissolved dyes are supposed: (i) charge neutralization through the binding of negatively charged pollutants with cationic hydrolysis products, and/or polymeric cations resulting in the reduction of their solubility and (ii) enmeshment or adsorption of pollutant molecules on metal hydroxide precipitates, also known as "sweep flocculation" mechanism.

In [11], the authors proposed enmeshment of dyes on iron oxide/hydroxide precipitates as the main mechanism of the removal of Reactive Red 43 with iron electrodes, due to existence of lag time between the process starting and reactive dye removal and negligible effect of initial pH.

However, other authors observed different mechanisms or side reactions, such as [28] who noted, besides sweep flocculation, degradation of the Reactive Red 43 as a minor pathway, proposing electrochemical reduction of dye and electro-Fenton as minor side reactions occurred in EC-Fe process. Another degradation mechanism was proposed by [29] for Reactive Black 5 using iron anode, in which vinyl sulfone was detected as one of the EC products, indicating reduction of azo bonds through oxidation of Fe^{2+} as the major step of decolorization.

Several studies have been carried out using electrocoagulation for the treatment of textile effluents, generally obtaining efficiencies above 90% [11,21,25,30–32].

Despite its advantages, electrocoagulation is not a consolidated technology yet, due mainly to the lack of a quantitative understanding of the complex process and its mechanisms and of a methodology for reactor design [33,34]. Through modeling of electrocoagulation processes, it is possible to build knowledge regarding theses aspects [22]; thus, studies have being conducted with the aim of modeling the various aspects of the process [35–38]. Among these studies, the kinetic analysis for pollutant removal stands out [39–41].

Among the possible models applied to describe the kinetics of the process, two types stand out: adsorption models and sigmoidal models. Adsorption models are most frequently applied to model electrocoagulation [42–45], due to one of the proposed mechanisms for the process was based on pollutant adsorption by coagulant ions produced (considered as adsorbents) [42]. These models also consider that the rate of pollutant removal is proportional to the mass ratio between the amount of the adsorbed species and adsorbent in the solution, and its relation to the values of those variables on equilibrium [46].

Sigmoidal models are generally used to describe growth phenomena, in which a limit or level of saturation is present [47], as well as the maximum removal of a pollutant in a treatment system. For this reason, sigmoidal curves are those that present continuous growth between two horizontal asymptotes, while passing through a single point of

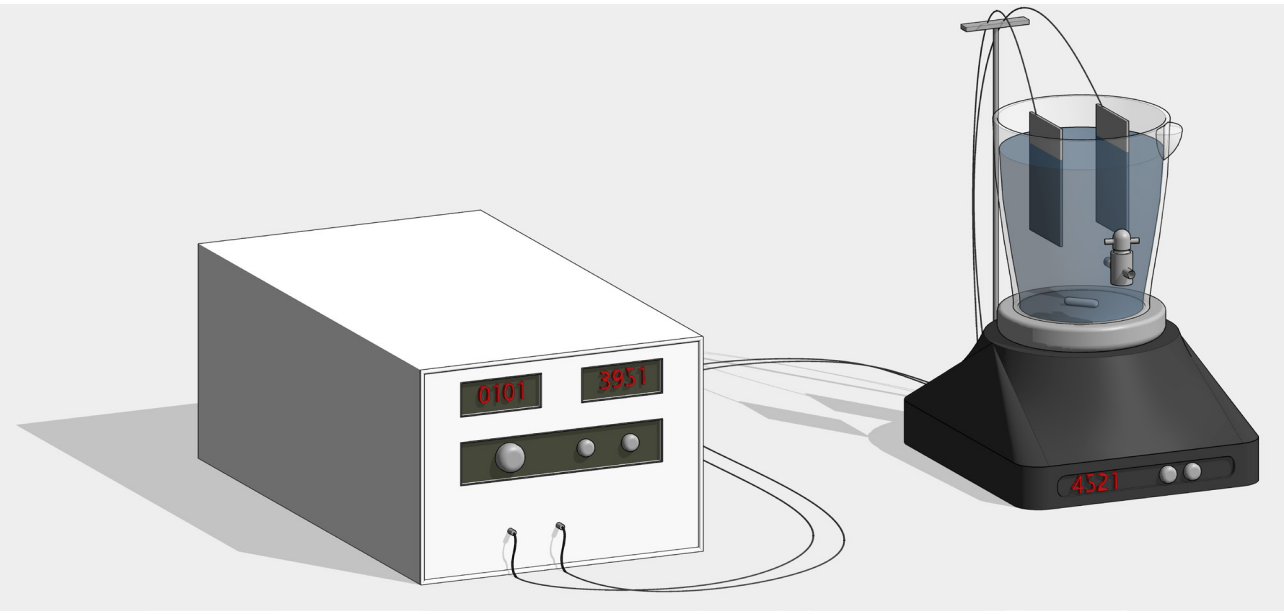

Fig. 1. Batch experimental system.

inflection [47,48].These curves are employed in some studies to model the kinetics of effluent treatment by adsorption [49], including dye removal [50,51] and other aspects of electrocoagulation, such as the evolution in flake diameter [52] and the rate of electrocoagulation [53].

The main contribution of this work was to obtain a model for the kinetics of reactive Blue 5G dye removal from synthetic effluent by electrocoagulation with iron electrodes. In addition to the evaluation of the adsorption and sigmoidal models on experimental data fitting, the kinetic model was validated experimentally, which is an important step for allowing its use in electrochemical reactors modeling and simulation.

Table 1
Characteristics of batch tests

Effluent volume per batch	1 L
Treatment time	240 s (testsA-E); 180 s (tests F-Z)
Immersed electrode area	0.0033 m²
Electrode length	33 cm²
Electrode height	11 cm
Electrode width	0.06 cm
Electrode format	Rectangular
Distance between electrodes	5 cm
Test temperature	25°C
Sample collection interval	40 s (tests A-E); 20 s (testsF-Z)
Concentration of NaCl in solution	5 g·L $^{-1}$

Table 2
Matrix of batch experiments

Electric current intensity (A)	Initial dye concentration (mg·L^{-1})				
	10.00	20.00	30.00	40.00	50.00
1.00	A	B	C	D	E
2.00	F	G	H	I	J
3.00	K	L	M	N	O
4.00	P	Q	R	S	T
5.00	U	V	X	Y	Z

2 Materials and methods

2.1. Materials

A textile company in Brazil supplied the reactive Blue 5G dye used in this work. The reactive Blue 5G dye belongs to the azo group of monochlorotriazine reactive dyes [54] and has a solubility greater than 100 g·L^{-1}at 25°C, a pH between 6.0 and 9.0, and a molar mass of 815 g·mol^{-1} [55]. The solution used as effluent was prepared by dissolving certain amounts of dye in distilled water, adding sodium chloride at a concentration of 5 g·L^{-1} in order to adjust the conductivity of the solution (7.00 ± 0.56 mS·cm^{-1}).

2.2. Experimental procedures

Tests were performed in duplicate utilizing a batch electrocoagulation system with two iron electrodes (anode/cathode). The textile effluent consisted of a solution of reactive Blue 5G dye and sodium chloride.

The system used in the tests is shown in Fig. 1.

Tests conditions were based on previous works [32] and preliminary tests, and are described in Table 1.

The tests had, as variables, the initial concentration of dye in the effluent and the intensity of electric current applied to the electrodes, while dye and iron concentrations were determined by samplings taken over time.

The matrix of experiments is described in Table 2.

Samples were left to settle in test tubes for about 12 h. In order to determine the dye concentration, the absorbance values were read in duplicate for each sample, in a molecular absorption spectrophotometer UV-Vis (Hach), at 618 nm wavelength. The samples digestion was carried out through direct heating in nitric acid. After that, iron concentration was determined since iron weight is considered as a variable in the kinetic adsorption models. In order to determine iron concentration, the absorbance was performed in an atomic absorption spectrophotometer (Varian, "AA240FS" model) with air-acetylene flame. The residual iron and dye concentrations were calculated using previously adjusted calibration curves for each species.

2.3. Kinetic modeling

2.3.1. Adsorption models

Pseudo-first-order and pseudo-second-order adsorption models, which are presented in Table 3, were tested for experimental data fit.

Table 3
Adsorption models tested

Adsorption model	Model[a]	Linearized model	Plotted variables	Fitted parameters
Pseudo-first order[a]	$\frac{dq}{dt} = kq$	$\log(q) = \log q_e - \frac{k\,t}{2{,}303}$	$\begin{pmatrix} t, \\ \log(q) \end{pmatrix}$	k q_e
Pseudo-second order[a]	$\frac{dq}{dt} = kq^2$	$\frac{t}{q_t} = \frac{1}{\left(kq_e^{\,2}\right)} + \frac{t}{q_e}$	$\left(t, \frac{t}{q_t}\right)$	k q_e

[a][42]

where t is the time (s); k is the kinetic rate constant of the reaction; and q_t [Eq. (5)] and q_e [Eq. (6)] correspond to the mass ratio quantities of adsorbed dye and adsorbent, on time and equilibrium stage, respectively.

$$q_t = \frac{V\left(C_0 - C_t\right)}{m_t}(5) q_e = \frac{V\left(C_0 - C_e\right)}{m_e} \quad (6)$$

where V is the volume of treated effluent (L); C_t the concentration of dye and m_t the adsorbent weight. The "0" and "e" indexes indicate the initial instant and the equilibrium, respectively.

Overall, the electrochemical dissolution mechanism of iron anodes reported in the literature is not consistent and lack an experimental proof of the actual species formed during EC [20]. Two main mechanisms for the production of the metal hydroxide have been proposed, and are presented in Eqs. (7)–(14) [18]:

Mechanism 1:

$$Fe \rightarrow Fe^{2+} + 2e \quad (7)$$

$$Fe^{2+}_{(aq)} + 2OH^-_{(aq)} \rightarrow Fe(OH)_{2(s)} \quad (8)$$

$$2H_2O_{(l)} + 2e^- \rightarrow 2OH^-_{(aq)} + H_{2(g)} \quad (9)$$

$$Fe_{(s)} + 2H_2O_{(l)} \rightarrow Fe(OH)_{2(s)} + H_{2(g)} \quad (10)$$

Mechanism 2:

$$4Fe \rightarrow 4Fe^{2+} + 8e \quad (11)$$

$$4Fe^{2+}_{(aq)} + 10H_2O_{(l)} + O_{2(g)} \rightarrow 4Fe(OH)_{3(s)} + 8H^+_{(aq)} \quad (12)$$

$$8H^+_{(aq)} + 8e^- \rightarrow 4H_{2(g)} \quad (13)$$

$$4Fe_{(s)} + 10H_2O_{(l)} + O_{2(g)} \rightarrow 4Fe(OH)_{3(s)} + 4H_{2(g)} \quad (14)$$

Table 4
Sigmoidal models tested

Model	Expression	
Logistic	$x = \frac{a}{1 + e^{-k(x-b)}}$	(15)
Richards	$x = \frac{a}{1 + e^{(b-kt)^{\frac{1}{s}}}}$	(16)
Weibull	$x = a - (a-b)e^{-(kt)^s}$	(17)

Source: Adapted from [47]

Iron(III) hydroxide, $Fe(OH)_3$, was considered as adsorbent. According to [56], it is the species found in greatest proportion in the pH range in which the treatment occurs (5.0–7.0). In this way, the mass of $Fe(OH)_3$ (m_t or m_e) was calculated based on the experimental determination of total iron concentration.

Subsequently, polynomial models for the values of k and q_e were obtained as functions of the variables: electric current intensity applied to the electrodes and initial concentration of dye. The fitting was performed using the *Curve Fitting Toolbox* of software MATLAB®v.R2013b.

2.3.2. Sigmoidal models

For the sigmoidal models, the variables used for fitting were time and the dimensionless ratio $C \cdot C_0^{-1}$. Table 4 shows the three sigmoidal models that were tested.

where b and s are parameters related to the position of the inflection point for each curve and k is the variation rate at the inflection point, thus corresponding to the kinetic constant. The parameter a is the value of the upper asymptote of the dependent variable, thus, it was set at 1 for all models, as this is the maximum value for the $C \cdot C_0^{-1}$ ratio.

The fittings were conducted separately for the data sets related to each value of current applied to the electrodes, in order to obtain, for each fitting, a value for the kinetic parameters.

Subsequently, a linear model was fitted for each parameter as a function of density of current ($A \cdot m^{-2}$) applied to the electrodes. In this way, it is possible to include in the model the influence of varying the current applied to the electrodes. The fitting was made as a function of density of current, rather than applied current (A), since it is the most usual parameter used in electrocoagulation studies [25,30,57].

2.4. Experimental validation

Validation tests were carried out in order to verify the predictive capacity of the models whose fitting was satisfactory. The tests were performed with the same conditions as those for the adjustment, except the electrical current applied to the electrodes and the initial dye concentration. For these variables, the conditions adopted are described in Table 5.

2.5. Thermodynamic analysis

The entropy generated in the process (S_{ger}) was estimated for the extreme conditions of applied current (1A

Table 5
Test conditions for kinetic model validation

Test	Initial dye concentration ($mg \cdot L^{-1}$)	Applied electric current (A)	Sampling interval (s)
1	32.1	0.5	40
2	40.4	1.5	20
3	38.4	2.5	20

and 5A) and the upper limit for initial dye concentration (50 mg·L^{-1}). The process was defined as a closed system, so it included the amount of iron dissolved from the electrodes. Since the temperature is constant, and variation for kinetic and potential energies, as well as volume, are negligible, for an adiabatic system the first law of thermodynamics for the process can be written [Eq. (18)]:

$$\int_0^{W_t} dW = \Delta U = \Delta H \tag{18}$$

The two sources of mechanical energy applied to the process were current applied to the electrodes and the magnetic agitation, so the equation can be rewritten as Eq. (19):

$$\int_0^{W_t} dW = V_{ps} It + P_{ma} t = \Delta U = \Delta H \tag{19}$$

where V_{ps} is the tension of the power source used to feed current to the electrodes, I is the applied current to the electrodes, P_{ma} is the power of the magnetic agitator, and t is the time of reaction, for which was considered the time required to attain 90% of removal. For constant pressure processes, the Maxwell´s relations establish that:

$$\left(\frac{\partial H}{\partial S}\right)_p = T or \frac{\Delta H}{\Delta S} \cong T \tag{20}$$

Using Eq. (20) in (19), and knowing that there is no heat exchange, so that ΔS is equal to the entropy generated in the process, it was possible to estimate it through Eq. (21) which is the generated entropy (S_{gen}):

$$\Delta S \cong \frac{V_{ps} It}{T} + \frac{P_{ma} t}{T} \tag{21}$$

Since the term relative to the magnetic agitator is equal for all conditions of applied current, and it was not possible to acquire reliable data for the actual power of the magnetic agitator, since it did not possess a voltage meter, the analysis was carried out only for the entropy produced due to the current fed to the electrodes. The parameters used are presented in Table 6.

The results were plotted in graphs of S_{ger} (J/K) for mass of dye removal (mg).

Evidently, the above equations also allow for the calculation of the entropy rate production. Since there is no change in the terms V_{ps}, I or W_{ma} along the process, the entropy rate production per second corresponds to the result of Eq. (21) when time is equal to 1 s. This result can also be used to provide information about the process, using an adaptation of the equations presented by Xie and Yu [58].

Table 6
Parameters for Thermodynamic analysis for initial dye concentration of 50 mg·L^{-1}

	Temperature, T (K)	Tension of power source, V_{ps} (V)	Time for 90% removal, t (s)
1 A	298	6,9	360
5 A	298	30,5	120

The equation of rate of change in entropy can be written as [58]:

$$\frac{dS}{dt} = \frac{\partial S}{\partial N}\frac{dN}{dt} + \frac{\partial S}{\partial U}\frac{dU}{dt} + \frac{\partial S}{\partial V}\frac{dV}{dt} \tag{22}$$

where N is the number of particles in the thermodynamic system, which decreases with coagulation. Since the system is considered closed, for mass conservation the particle volume remains constant. The corresponding rate of change dV/dt is zero. According to the thermodynamic identification, the relationship between entropy and internal energy is:

$$\left(\frac{\partial S}{\partial U}\right)_V = \frac{1}{T} \tag{23}$$

The internal energy can be considered as the sum of kinetic energy and surface free energy, so that:

$$\frac{dU}{dt} = \frac{dk_e}{dt} + \sum_{i=1}^{2} \sigma_i \frac{ds_i}{dt} \tag{24}$$

where k_e is the total kinetic energy of the system, s is the particle surface energy for each species (iron and dye), and s is the total particle surface for each species. Since the system is under agitation, for this analysis only the kinetic energy relative to particle advection will be considered, so that the kinetic energy of a particle relates to its mass and the velocity gradient in the reactor due to agitation. Since agitation rate is constant, the term for kinetic energy rate of change is also considered zero. Eq. (24) tell us, therefore, that internal energy variation rate is proportional to particle surface energy and total particle surface.

According to [58], the change of free energy in a thermodynamic system with respect to the change in the number of molecules is defined as the chemical potential of the disperse system, and is typically calculated as:

$$\frac{\partial S}{\partial N} = -k_B \ln\left(N\lambda_{th}^3\right) \tag{25}$$

where k_B is the Boltzmann constant, and λ_{th} the thermal wavelength.

Based on the equations above, the rate of change for entropy for the system can be expressed as:

$$\frac{\partial S}{\partial t} = -k_B \ln\left(N\lambda_{th}\right)\frac{dN}{dt} + \frac{\sigma}{T}\frac{ds}{dt} \tag{26}$$

The change of rate in the number of particles refers to both the dissolution of iron in the liquid phase and the reduction in particle number due to coagulation. Also, the total particle surface (s) for each species is also a function of the number of particles of each species, and decreases with an increase in the average particle volume (in other words, decreases with coagulation) [58]. Since the entropy generation was calculated, the analysis of these tendencies based on Eq. (26) and thermodynamic theory allows to obtain some information about the process, which will be presented in the results.

3. Results and discussion

3.1. Batch experiments

The average values of dye concentration over time were compiled in graphs (Fig. 2), according to the electrical current intensity applied to the electrodes.

By analyzing the decay of dye concentration over time, it is observed that the reaction approaches the equilibrium at the end of the sampling time. It is also observed that the rate of dye removal, in relation to time, varies according to the current applied to the electrodes. In general, an increase in the applied current causes an increase in the reaction rate.

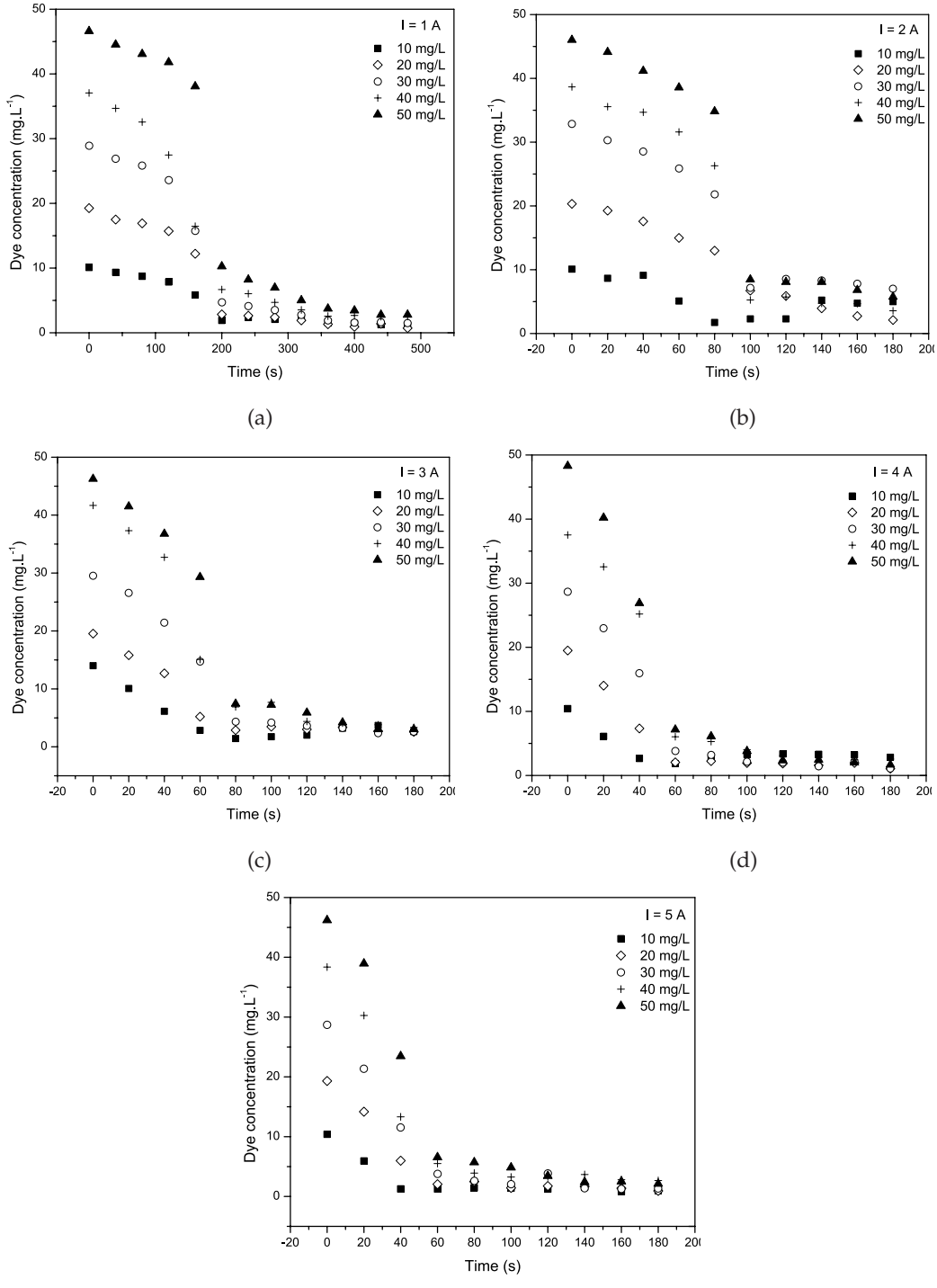

Fig. 2. Dye concentration as a function of time for the tests with electric current intensity of (a) 1A; (b) 2A; (c) 3A; (d) 4A; (e) 5A.

Furthermore, the reaction rate changes over time for the same condition, so that a $t_i at_{i+n}$ interval is observed between two samplings, in which there is a maximum decay, and a removal of a significant amount of dye in a short period of time. The beginning (t_i) of this abrupt decay tends to vary according to the applied current, occurring sooner as the current increases. In tests with an electric current intensity of 1A, decay occurred between 160 and 200 s; in tests with an intensity of 2A, between 80 and 100 s; with an intensity of 3A, between 60 and 80 s; and for intensities of 4A and 5A, between 40 and 60 s.

These results are in accordance with those obtained by [11] who, similarly, studied dye removal through electrocoagulation using iron electrodes. The authors observed three stages in the process: a lag period between the beginning of the process and the start of significant dye removal (where the lag time decreases with increasing current); a reactive period in which the removal increased rapidly; and a period of stability in the removal of the dye. [58] found similar results, although they studied the removal of clay-based pollutants. It is also possible to observe that, in general, the dye concentration decay over time presents a behavior similar to that of the sigmoidal curves.

3.2. Fitting kinetic data to experimental data

3.2.1. Kinetic adsorption models

The adjustment test of adsorption models described in Eqs. (1) and (3) resulted in a value for the kinetic constant (k) for each experiment. Table 7 shows the values of k and R^2 for each adjustment, as well as the value of q_e and $[Fe]_e$ (iron concentration at equilibrium) observed for each test.

For most of the tests, a good fitting was obtained for both models (in most cases R^2 values were above 90%). Moreover, the values of k generally proved to be consistent, except for a few tests where the values of k were negative.

In this way, a model for k for each of these fittings was obtained in addition to the model for q_e. The model for the first order kinetics was obtained as a function of the current applied to the electrodes, and the model for the second order kinetics as a function of the current applied and the initial dye concentration. For the fittings of both models, the tests that obtained R^2 above 85% and positive k were selected. The fitting obtained for the first-order model is described in Eq. (27).

$$k_1 = 0.0026I^2 - 0.0199I + 0.0051 \quad (27)$$

Table 7
Adjustments for the adsorption models

Ensaio	q_e (mg·g^{-1})	$[Fe]_e$ (mg·g^{-1})	Pseudo 1ª order		Pseudo 2ª order	
			k (min^{-1})	R^2	k (g·mg^{-1}·min^{-1})	R^2
A	31.61	86.53	0.00952	96,67	0,00211	93,27
B	65.10	84.20	0.01163	93,78	0,00161	89,01
C	96.27	84.25	0.01276	94,18	0,00088	86,67
D	146.01	84.36	0.01408	86,63	–0,000807	86,68
E	154.50	71.20	0.01248	91.77	–0.000122	68.09
F	47.74	119.73	0.04039	88.86	–0.002175	75.73
G	85.30	86.53	0.01965	84.59	–0.000876	96.13
H	148.31	85.60	0.02654	82.61	–0.000399	85.96
I	164.40	88.66	0.02563	87.23	–0.000277	83.47
J	188.61	82.70	0.02655	86.51	–0.00018	69.99
K	58.95	164.17	0.03578	93.58	0.0035	98.10
L	68.49	173.87	0.03078	84.41	0.00146	95.43
M	84.07	144.95	0.03061	92.07	0.00097	90.61
N	107.60	130.69	0.03159	95.77	0.00073	92.53
O	136.31	134.76	0.02875	92.65	0.00102	92.16
P	26.79	104.37	0.05949	94.70	0.00439	95.90
Q	43.15	200.10	0.02735	95.9	0.00119	92.35
R	64.56	221.58	0.03468	95.44	0.00078	91.32
S	81.89	150.97	0.03428	93.73	0.00045	93.10
T	109.13	95.56	0.03253	97.60	0.00046	92.58
U	17.66	178.07	0.03134	97.74	0.00335	92.64
V	60.30	246.12	0.0559	89.83	0.00197	92.67
X	52.10	159.38	0.02661	94.22	0.00084	93.14
Y	100.85	176.66	0.0419	97.68	0.00049	93.42
Z	82.55	142.17	0.0314	97.18	0.00059	92.62

Eq. (18) showed an R^2 equal to 91.38%.

The model for second order kinetics resulted in an R^2 equal to 90.86%, and is described in Eq. (28).

$$k = -0.006245 + 0.0003114C_0 - 0.000328I - 4.06x10^{-6}C_0^2 + 2.81210^{-6}IC_0 + 4.434x10^{-5}I^2 \quad (28)$$

Based on the experimental data and the q_e value observed for each test, a model was also adjusted for this parameter as a function of the variables: electrical current intensity applied to the electrodes and initial dye concentration in the solution. The model resulted in an R^2 value equal to 95%, and is described in Eq. (29).

$$qe = -123.1 + 2.929C_0 + 174.5I + 0.05833{C_0}^2 - 0.4059IC_0 - 62.64I^2 - 0.00076{C_0}^3 - 0.00057{C_0}^2I - 0.0097C_0I^2 + 6.664I^3 \quad (29)$$

3.2.2. Fitting with sigmoidal models

Table 8 shows the R^2 coefficients for the fittings with sigmoidal models, which were carried out with data from experiments conducted for each value of applied current.

Satisfactory adjustments were obtained for the Logistic and Weibull models. Once the values for the kinetic parameters for each current density (j) value were obtained, a linear fitting for each parameter of the two models was performed as a function of *j*. The R^2 values for each fitting are shown in Table 9.

Despite the good fittings for the *k* parameter for the Weibull curve, it was not possible to obtain a model as a function of *j* for the *b* parameter. In this way, among the sigmoidal models tested, the Logistic model proved to be the best option to represent the kinetics of the removal of the reactive Blue 5G dye by electrocoagulation. Fig. 3 shows the fittings of experimental data for each electrical current intensity evaluated (R^2 are listed in Table 7).

Table 8
Determination coefficients for the sigmoidal models

Current intensity (A)	Logistic	Weibull	Richards
1	0.94794	0.9481	0.9471
2	0.92952	0.9170	Fit failed
3	0.92216	0.8969	Fit failed
4	0.93142	0.8894	Fit failed
5	0.92329	0.9473	Fit failed

Table 9
R^2 values of the adjusted models for parameters of the sigmoidal models

Parameter	Logistic	Weibull
k^1	0.9959	0.9778
b^2	0.9894	0.3347
s^1	–	0.8346
a^3	–	–

[1]First-order linear model; [2]Second-order polinomial model
[3]Parameter value fixed at 1

The model for the value of *k* as a function of *j* is shown in Eq. (30):

$$\frac{\partial S}{\partial t} = -k_B \ln\left(N\lambda_{th}\right)\frac{dN}{dt} + \frac{\sigma}{T}\frac{ds}{dt} \quad (30)$$

3.3. Experimental validation

Validation was carried out for adsorption and logistic. The predicted and observed concentration results for the validation tests are shown in Fig. 4.

It may be noted that the adsorption models did not present a satisfactory performance, since the values predicted by these models were very different from the experimental results. The fitted Logistic model, in turn, was able to predict the variation of the dye concentration over time for the batch system with a greater accuracy.

Thus, among those tested, the Logistic model proved to be the best to describe the kinetics of reactive Blue 5G dye removal by electrocoagulation, and the comparison between the experimental and simulated data proved its validity.

The poor performance of the adsorption models, which consider the amount of iron present in the solution, possibly indicates that, for the process studied, the generation of coagulating ions is not a determining step in dye removal rate.

3.4. Thermodynamic analysis

Table 10 contains the entropy generated at 90% dye removal for both conditions.

For the same efficiency of treatment, the entropy generated was much greater for the applied current of 5A than for 1A. This indicates that the sustainability of the process is greater for milder conditions, even though it takes longer to attain the same level of treatment. It should be noted that the choice of operation conditions should also take into account the desired removal rate, which is faster for higher currents.

Fig. 5 shows the graphs for entropy generated, Sger (J/K) per mass of dye removed (mg).

The graphs show abrupt changes in the inclination of the curves, which are in agreement with the behavior observed in the kinetic modeling. On the other hand, the entropy generation rate for this process appears to be constant (i.e. there are no peaks in entropy generation that could justify the abrupt decay). Eq. (26) (repeated below) shows that entropy generation rate is a function of the number of particles or molecules of a thermodynamic system and the change in particle specific surface area.

$$\frac{\partial S}{\partial t} = -k_B \ln\left(N\lambda_{th}\right)\frac{dN}{dt} + \frac{\sigma}{T}\frac{ds}{dt} \quad (26)$$

Here a distinction from conventional coagulation has to be made, since in electrocoagulation, there are other phenomena that change particle number besides the formation of flocs: dissolution of electrodes and gas production. Since there is a continuous incorporation of particles in the system, which not only gain kinetic energy they did not possess before hand, but also increase their surface area, which, by Eq. (26), causes increase in free surface energy. Coagulation,

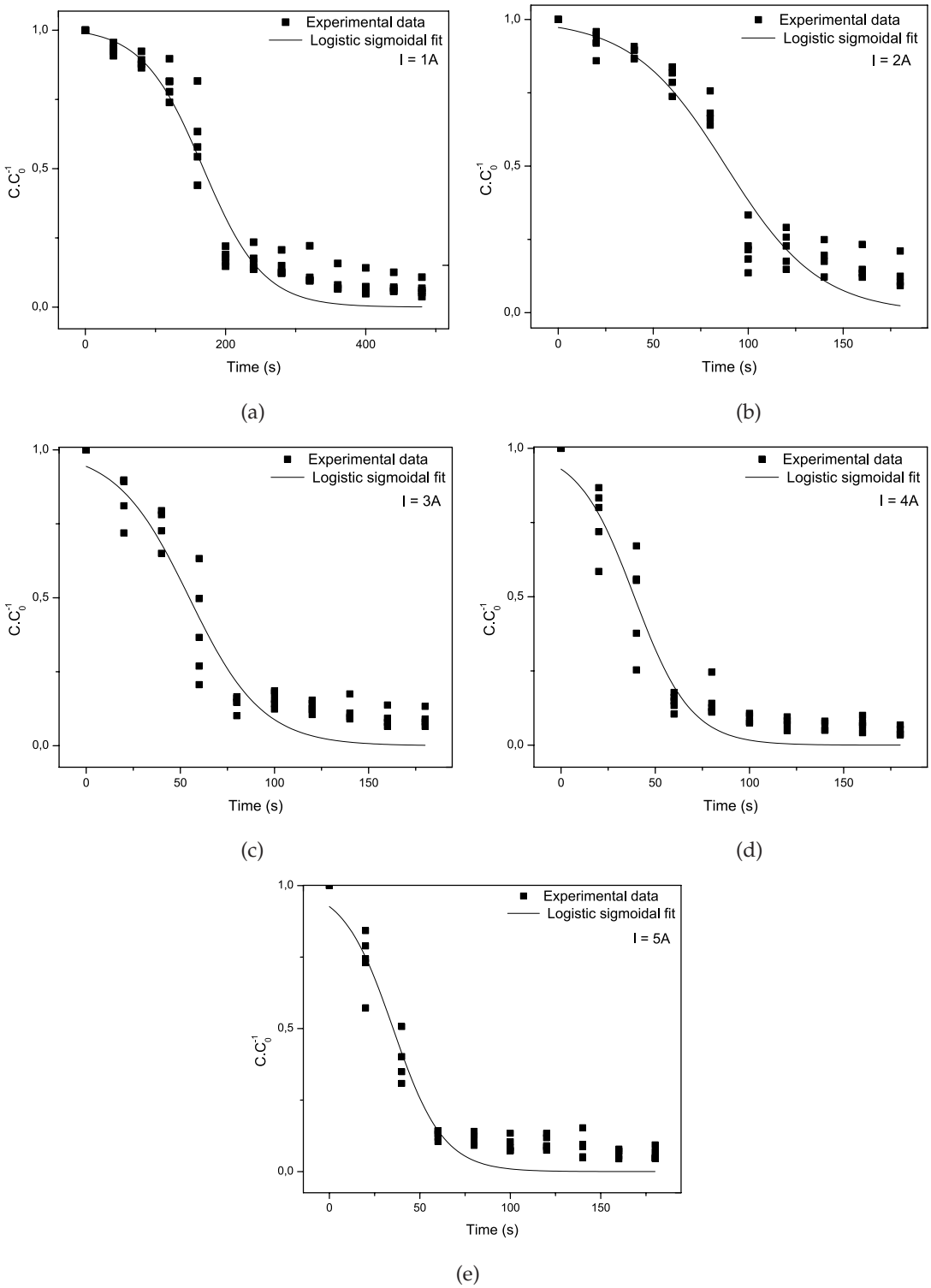

Fig. 3. Kinetic fittings for the sigmoidal logistic model of experiments with current equal to (a) 1A, (b) 2A, (c) 3A, (d) 4A, (e) 5A.

on the other hand, represents both a reduction in particle number as well as in total particle specific surface area.

When the thermodynamics of the process is considered, it may be adequate to ask why does flocculation occur at all, given that one could suppose that the agglomeration of particles will lead to less possible microstates, implying a reduction in entropy, which does not occur spontaneously in closed processes, as the second law of thermodynamics states. Although whether the number of microstates increases or decreases with coagulation in this particular

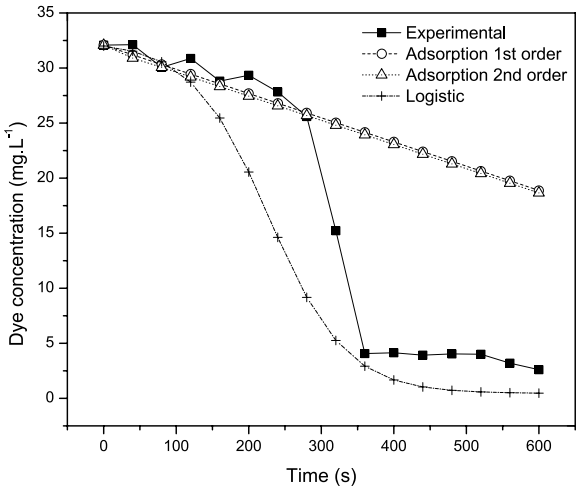

(a)

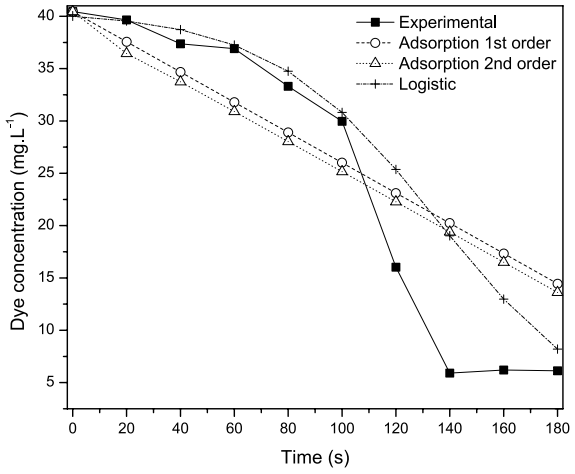

(b)

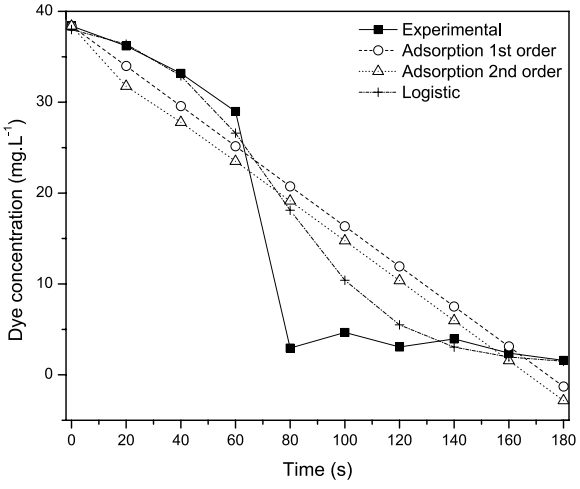

(c)

Fig. 4. Dye concentration observed and predicted with the adsorption and sigmoidal models for the tests (a) 1; (B) 2; (C) 3.

Table 10
Entropy generation at 90% for 1 and 5 A

Current, I (A)	Entropy, Sger (J/K)
1	8.33
5	61.41

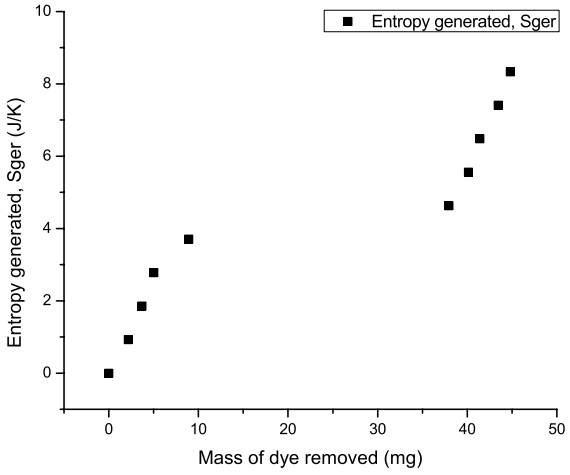

(a)

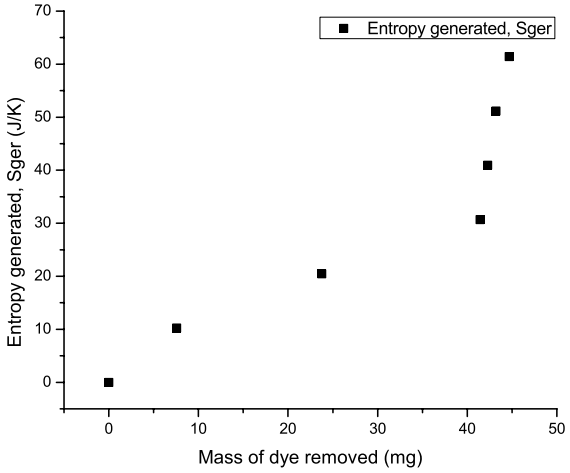

(b)

Fig.5. Entropy generated (J/K) per mass of dye removed (mg) for current of(a) 1A (b) 5A.

process is certainly debatable (states that the proximity of a polymer and a colloid would allow for more possible configurations, increasing entropy, for instance; and the long chained dye molecules could, perhaps, characterize as such), this can also be understood looking at another thermodynamic concept.

As it is well known [59], the second law of thermodynamics also implies that, in a not isolated system, it will tend to minimize its Helmholtz free energy $F = U - TS$, where U is the internal energy of the system, T the temperature and S

the entropy. For a system at constant temperature, there are two ways to lower its free energy: by increasing entropy, or by decreasing internal energy.

For this process, as calculated, the entropy is constantly increasing as long as there is electric current flowing – in other words, the second derivative of entropy generation is null. So for the free energy of the system to reach a minimum, it leaves only minimization of internal energy. As stated previously, and according to Eq. (24), internal energy can be understood as the sum of kinetic energy and surface free energy [58].

This fact explains why coagulation occurs, since the aggregation on particles it represents both a reduction in specific surface area (which decreases with an increase in average particle volume [58]), as well as in kinetic energy. According to Xie and Yu [58], in the classical theory of coagulation, coalescence occurs instantaneously after two particles collide and the time scale of the collision of two particles is far smaller than the time scale of particle number evolution. Therefore, according to the author, Brownian coagulation could be considered a perfectly inelastic collision process because kinetic energy is not conserved due to the action of internal friction. In a perfectly inelastic collision, the colliding particles stick together and the maximum amount of kinetic energy of the system is lost. This implies in maximum loss of free energy.

Also, it should be noted that the rate term for entropy generation being constant represents another constraint to the system. Since Eq. (26) is a sum of two terms, one that depends on number of particles, and the other that depends on total particle specific surface area, the sum of these terms has to be constant as well.

At the beginning of the process, before coagulation starts, the variation in particle number is due to dissolution of iron and bubble generation, and so both terms on the right are constant, while their sum is the entropy generation. The theory for coagulation shows, however, that the increasing number of ions will inevitably lead to the production and growth of flocs, since it increases the statistical chances of collision.

Looking at Eq. (26), it is easy to notice that when the first flocs are formed and the rate of variation in number of particles decreases, there must be a corresponding reduction of particle specific area. The equation can also be written so that particle specific surface area is a function of the number of particles:

$$k\frac{\partial S}{\partial t}=\frac{dN}{dt}\left(-k_B\ln\left(N\lambda_{th}\right)+\frac{\sigma}{T}\frac{ds}{dN}\right) \tag{31}$$

So, for this corresponding reduction to occur, the rate with which the surface area changes with respect to particle number variation must decrease. This can be achieved only if the particles become more and more agglomerated.

A possible explanation for the peak in dye decay could come from reasoning that, if the decrease in particle number due to coagulation ever outweighs the increase due to dissolution and electrolysis, the rate dN/dt becomes negative and the whole equation changes sign. In order for the system to obey the constraint for entropy generation, there has to be a corresponding and instantaneous reduction of particle specific area, which would be achieved by the abrupt increase in formation in flocs that is visible in the peak of dye decay.

This phenomenon could also explain why the adsorption models did not describe adequately the process, which was, in turn, well modeled by sigmoidal models. The adsorption process, in general, does not present abrupt changes in its kinetics. While the removal rate does change along the process, this is due to the continuous occupation of active sites. Electrocoagulation, on the other hand, at least for the process described in this paper, seems to be characterized for having a turning point in its process, where the maximum decay occurs suddenly and in a short period of time, as previously described.

Also, it is relevant to mention that the curves present characteristics that strongly suggest that a change in phase is occurring, due to the abrupt decay of pollutant with no correspondent change in entropy generation. That is in agreement with the classical view of the technology, which according to Bocos et al. (2016) [60], has long been considered a phase separation process.

4. Conclusions

The electrocoagulation aspects modeling, such as kinetic process, is extremely important for consolidation of this wastewater treatment technology. Several studies have been conducted in this regard; however, they rarely included experimental validation of the adjusted models. Such validation is a ruling factor in order to evaluate the actual predictive capacity of the adjusted model, thus determining whether it is, in fact, able to integrate the modeling and simulation of electrochemical reactors.

Experiments were conducted to remove reactive Blue 5G dye from a synthetic solution by electro coagulation, over a wide range of conditions for two variables: electrical current intensity applied to the electrodes (A) and initial dye concentration ($mg{\cdot}L^{-1}$). It was verified that the kinetics of removal of the reactive Blue 5G dye was influenced by the electric current intensity.

Among the models tested, the adsorption and sigmoidal models provided good adjustments. However, the validation of the models with new experimental conditions showed that the performance of the Logistic sigmoidal model was much superior than the adsorption models, which are more commonly used in the scientific literature. Thus, the validity of the proposed Logistic model is verified, as well as the possibility of using sigmoidal curves to model the kinetics of this complex phenomenon.

A thermodynamic analysis was also conducted with the experimental results, in which the entropy generation of the process was calculated and found to be a constant term. This analysis allowed to discuss electro coagulation mechanisms from the thermodynamic perspective of the process, as well as possible reasons for sigmoid models presenting a better fit than the usually employed adsorption curves, which are related to the process, in this case, presenting a turning point in its efficiency as a defining characteristic.

Acknowledgments

This work was supported by FUNDAÇÃO ARAUCARIA and CAPES (Coordenação de Aperfeiçoamento de Pessoal de Nível Superior) [grant numbers 44519.450.39962.11082014].

Symbols

C_0 — Initial concentration of dye
C_t — Concentration of dye with time
P_{ma} — Power of magnetic agitator
S_{ger} — Entropy generated
V_{ps} — Tension of power source
k_B — Boltzmann constant
k_e — Total kinetic energy of the system
m_t — Adsorbent weight
q_e — Mass ratio quantity of adsorbed time and adsorbent on equilibrium
q_t — Mass ratio quantity of adsorbed time and adsorbent with time
λ_{th} — Thermal wavelength
H — Enthalpy
I — Current applied to the electrodes
N — Number of particles in the thermodynamic system
S — Entropy
T — Temperature
U — Internal energy
V — Volume of treated effluent
W — Work
a — Value of upper asymptote of the dependent value for sigmoid curves
b — Parameter related to the position of inflection point for sigmoid curves
j — Current density applied to the electrodes
k — Kinetic rate constant of the reaction
s — Total particle surface for the species
s — Parameter related to the position of inflection point for sigmoid curves
t — Time of reaction
s — Surface free energy for the species

References

[1] E.K. Morali, N. Uzal, U. Yetis, Ozonation pre and post-treatment of denim textile mill effluents: Effect of cleaner production measures, J. Cleaner Prod., 137 (2016) 1–9.
[2] L. Chen, L. Wang, X. Wu, X. Ding, A process-level water conservation and pollution control performance evaluation tool of cleaner production technology in textile industry, J. Cleaner Prod., 143 (2017) 1137–1143.
[3] C. Phalakornkule, S. Polgumhang, W. Tongdaung, B. Karakat, T. Nuyut, Electrocoagulation of blue reactive, red disperse and mixed dyes, and application in treating textile effluent, J. Environ. Manag., 91 (2010) 918–926.
[4] V. Khandegar, A.K. Saroha, Electrochemical treatment of textile effluent containing acid Red 131 dye, J. Hazard. Toxic Radioact. Waste., 18(1) (2014) 38–44.
[5] C.D. Raman, Textile dye degradation using nano zero valent iron: A review, J. Environ. Manage., 177 (2016) 341–355.
[6] G.T. Guyer, K. Nadeem, D. Nadir, Recycling of pad-batch washing textile wastewater through advanced oxidation processes and its reusability assessment for Turkish textile industry, J. Cleaner Prod., 139 (2016) 488–494.
[7] M.A. Ubale, V.D. Salkar, Experimental study on electrocoagulation of textile wastewater by continuous horizontal flow through aluminum baffles, Korean J. Chem. Eng., 34, (2017) 1044–1047.
[8] B.K. Korbahti, A. Tanyolac, Electrochemical treatment of simulated textile wastewater with industrial components and Levafix Blue CA reactive dye: Optimization through response surface methodology, J. Hazard. Mater., 151 (2008) 422–431.
[9] M. Kobya, E. Gengec, E. Demirbas, Chem. Eng. Process., 101 (2016) 87–100.
[10] T. Saraswathy, A. Singh, S. Ramesh, S. Thanga, New trends in Electrocoagulation for the removal for dyes from wastewater: A review, Environ. Eng. Sci., 30(7) (2013) DOI: 10.1089/ees.2012.0417.
[11] A.R. Amani-Ghadim, A. Olad, S. Aber, H. Ashassi-Sorkhabi, Comparison of organic dyes removal mechanism in electrocoagulation process using iron and aluminum anodes, Environ. Prog. Sustain. Energy, 32(3) (2013) 547–556.
[12] A. Bafana, S.S. Devi, T. Chakrabarti, Azo dyes: past, present and the future, Environ. Rev., 19 (2011) 350–371.
[13] T.H. Kim, C. Park, E.B. Shin, S. Kim. Decolorization of disperse and reactive dyes by continuous electrocoagulation process, Desalination, 150 (2002) 165–175.
[14] B. Merzouk, K. Madani, A. Sekki, Using electrocoagulation-electroflotation technology to treat synthetic solution and textile wastewater, two case studies, Desalination, 250 (2010) 573–577.
[15] H. Kusic, N. Koprivanac, L. Srsan, Azo dye degradation using Fenton type processes assisted by UV irradiation: A kinetic study, J. Photochem. Photobiol. A: Chem., 181 (2006) 195–202.
[16] S. Singh, V.C. Srivastava, I.D. Mall, Mechanistic study of electrochemical treatment of basic green 4 dye with aluminum electrodes through zeta potential, TOC, COD and color measurements, and characterization of residues, RSC Adv., 3 (2013) 16426–16439.
[17] A. Akyol, Treatment of paint manufacturing wastewater by electrocoagulation, Desalination, 285 (2012) 91–99.
[18] N. Daneshvar, A. Oladegaragoze, N. Djafarzadeh, Decolorization of basic dyes by electrocoagulation: An investigation of the effect of operational parameters, J. Hazard. Mater. B, 129 (2006) 116–122.
[19] N. Daneshvar, D. Salari, A.R. Khataee, Photocatalytic degradation of azo dye acid red 14 in water: investigation of the effect of operational parameters, J. Photochem. Photobiol. A, 157 (2003) 111–116.
[20] D.T. Moussa, M.H. El-Naas, M. Nasser, M.J. Al-Marri, A comprehensive review of electrocoagulation for water treatment: Potentials and challenges, J. Environ. Manag., 186 (2017) 24–41.
[21] B. Merzouk, M. Yakoubi, I. Zongo, J.P. Leclerc, G. Paternotte, S. Pontvianne, S. Pontvianne, F. Lapicque, Effect of modification of textile wastewater composition on electrocoagulation efficiency, Desalination, 275 (2011) 181–186.
[22] J.N. Hakizimana, B. Gourich, M. Chafi, Y. Stiriba, C. Vial, P. Drogui, J. Naja, Electrocoagulation process in water treatment: A review of electrocoagulation modeling approaches, Desalination, 404 (2017) 1–21.
[23] G. Chen, Electrochemical technologies in wastewater treatment, Sep. Purif. Technol., 38(1) (2004) 11–41.
[24] M.Y.A. Mollah, P. Morkovskyb, J. Gomesc, M. Kesmezc, J. Pargad, D.L. Cockec, Fundamentals, present and future perspectives of eletrocoagulation, J. Hazard. Mater., 114 (2014) 199–210.
[25] S. Zodi, B. Merzouk, O. Potier, F. Lapicque, J.P. Leclerc, Direct red 81 dye removal by a continuous flow electrocoagulation/flotation reactor, Sep. Purif. Technol., 108 (2013) 215–222.
[26] P. Cañizares, F. Martínez, C. Jiménez, J. Lobato, M.A. Rodrigo, Coagulation, electrocoagulation of wastes polluted with dyes, Environ. Sci. Technol., 40 (2006) 6418–6424.
[27] J. Duan, J. Gregory, Coagulation by hydrolysing metal salts, Adv. Colloid Interface Sci., 100–102 (2003) 475–502.
[28] A.R. Amani Ghadim, Optimization of electrocoagulation process for removal of an azo dye using response surface methodology and investigation on the occurrence of destructive side reactions, Chem. Eng. Process., 64 (2012) 68–78.
[29] U.D. Patel, J.P. Ruparelia, M.U. Patel, Electrocoagulation treatment of simulated floor-wash containing Reactive Black 5 using iron sacrificial anode, J. Hazard. Mater., 197 (2011) 128–136.
[30] B.K. Nandi, S. Patel, S. Effects of operational parameters on the removal of brilliant green dye from aqueous solutions by electrocoagulation, Arab. J. Chem., 10(2) (2017) S2961–S2968.

[31] E. Pajootan, M. Arami, N.M. Mahmoodi, Binary system dye removal by electrocoagulation from synthetic and real colored wastewaters, J. Taiwan. Inst. Chem. Eng., 43 (2012) 282–290.
[32] B.S. Santos, E. Eyng, P.R.S. Bittencourt, L.M. Frare, E.L. Flores, M.B. Costa, Electro-flocculation associated with the extract of Moringa oleifera Lam as natural coagulant for the removal of reactive blue 5G dye, Acta. Sci. Technol., 38(4) (2016) 438–444.
[33] W. Bouguerra, K. Brahmi, E. Elimame, M. Loungou, B. Hamrouni, Optimization of electrocoagulation operating parameters and reactor design for zinc removal: application to industrial Tunisian wastewater, Desal. Water Treat., 56(10) (2015) 2672–2681.
[34] P.K. Holt, G.W. Barton, C.A. Mitchell, The future for electrocoagulation as a localized water treatment technology, Chemosphere, 59(3) (2005) 355–367.
[35] P. Cañizares, C. Jiménez, F. Martínez, M.A. Rodrigo, C. Sáez, The pH as a key parameter in the choice between coagulation and electrocoagulation for the treatment of wastewaters, J. Hazard. Mater., 163 (2008) 158–164.
[36] K.L. Dubrawski, C. Du, M. Mohseni, General potential-current model and validation for electrocoagulation, Electrochim. Acta., 129 (2014) 187–195.
[37] A. Vázquez, I. Rodríguez, I. Lázaro, Primary potential and current density distribution analysis: A first approach for designing electrocoagulation reactors, Chem. Eng. J., 179 (2012) 253–261.
[38] A. Vázquez, J.L. Nava, R. Cruz, I. Lázaro, I. Rodríguez, The importance of current distribution and cell hydrodynamic analysis for the design of electrocoagulation reactors, J. Chem. Technol. Biotechnol., 89 (2014) 220–229.
[39] T. Yehya, M. Chafi, W. Balla, C. Vial, A. Essadki, B. Gourich, Experimental analysis and modeling of denitrification using electrocoagulation process, Sep. Purif. Technol., 132 (2014) 644–654.
[40] A.E. Yilmaz, R. Boncukcuoglu, M.M. Kocakerim, E. Kocadagistan, An empirical model for kinetics of boron removal from boron containing wastewaters by the electrocoagulation method in a batch reactor, Desalination, 230 (2008) 288–297.
[41] M.H. Isa, E.H. Ezechi, Z. Ahmed, S.R.M. Kutty, Boron removal by electrocoagulation and recovery, Water Res., 51 (2010) 113–123.
[42] K. Chithra, N. Balasubramanian, Modeling electrocoagulation through adsorption kinetics, J. Model. Simul. Syst., 1(2) (2010) 124–130.
[43] E.H. Ezechi, M.H. Isa, S.R.M. Kutty, A. Yaqub, Boron removal from produced water using electrocoagulation, Process Saf. Environ. Prot., 92 (2014) 509–514.
[44] A.N. Ghanim, S.K. Ajjam, Modeling of textile wastewater electrocoagulation via adsorption isotherm kinetics, Iraqi J. Mech. Mater. Eng., 13(1) (2013) 49–62.
[45] S. Vasudevan, J. Lakshmi, G. Sozhan, Electrochemically assisted coagulation for the removal of boron from water using zinc anode, Desalination, 310 (2013) 122–129.
[46] V. Khatibimakal, A. Torabiam, F. Janpoor, G. Hoshyaripour, Fluoride removal from industrial wastewater using electrocoagulation and its adsorption kinetics, J. Hazard. Mater., 179 (2010) 276–280.
[47] M. Carrillo, J.M. González, A new approach to modelling sigmoidal curves. Departamento de Economía Aplicada, Universidad de La Laguna, Tenerife, Canary Islands, Spain, 2002.
[48] A.H. Bilge, Y. Ozdemir, The Critical Point of a Sigmoidal Curve: The Generalized Logistic Equation Example, Cornell University, 2014.
[49] Q. Cai, B. Turner, D. Sheng, S. Sloan, The kinetics of fluoride sorption by zeolite: Effects of cadmium, barium and manganese, J. Contam. Hydrol., 177–178 (2015) 136–147.
[50] A. Çelekli, G. Ilguna, H. Bozkurt, Sorption equilibrium, kinetic, thermodynamic, and desorption studies of Reactive Red 120 on Characontraria, Chem. Eng. J., 191 (2012) 228–235.
[51] A. Çelekli, H. Bozkurt, Sorption and desorption studies of a reactive azo dye on effective disposal of redundant material, Environ. Sci. Pollut. Res., 20 (2013) 4647–4658.
[52] T. Harif, M. Khai, A. Adin, Electrocoagulation versus chemical coagulation: Coagulation/flocculation mechanisms and resulting floc characteristics, Water Res., 46 (2012) 3177–3188.
[53] M.J. Matteson, R.L. Dobson, R.W. Glenn, Jr., N.S. Kukunoor, W. H. Waits Iii, E.J. Clayfield, Electrocoagulation and separation of aqueous suspensions of ultrafine particles, Colloids Surf. A, 104 (1995) 101–109.
[54] N. Koprivanac, H. Kusic, D. Vujevic, B.R. Locke, Influence of iron on degradation of organic dyes in corona, J. Hazard. Mater., 117 (2005) 113–119.
[55] M.F. Klen, Adsorption kinetics of blue 5G dye from aqueous solution on dead floating aquatic macrophyte: effect of pH, temperature, and pretreatment, Water Air Soil Pollut., 223(7) (2012) 4369–4381.
[56] C. Barrera-Dias, F. Urena-Nunes, E. Campos, M. Palomar-Pardave, M. Romero-Romo, A combined electrochemical-irradiation treatment of highly colored and polluted industrial wastewater, Radiat. Phys. Chem., 67 (2003) 657–663.
[57] M.C. Wei, K.S. Wang, C.L. Huang, C.W. Chiang, T.J. Chang, S.S. Lee, S.H. Chang, Improvement of textile dye removal by electrocoagulation with low-cost steel wool cathode reactor, Chem. Eng. J., 192 (2012) 37–44.
[58] M. Xie, M. Yu, Thermodynamic analysis of Brownian coagulation based on moment method, Int. J. Heat Mass Transfer, 122 (2018) 922–928.
[59] P.K. Holt, G.W. Barton, M. Wark, C.A. Mitchell, A quantitative comparison between chemical dosing and electrocoagulation, Colloids Surf., 211(1) (2002) 233–248.
[60] E. Bocos, E. Brilas, N. Sanroma, I. Sire, Electrocoagulation: simply a phase separation technology? The case of Bronopol compared to its treatment by EAOPs, Environ. Sci. Tech., 50 (2016) 7679–7686.